



Deposited via The University of Leeds.

White Rose Research Online URL for this paper:

<https://eprints.whiterose.ac.uk/id/eprint/82923/>

Version: Accepted Version

---

**Article:**

Drew, DR, Barlow, JF and Cockerill, TT (2013) Estimating the potential yield of small wind turbines in urban areas: A case study for Greater London, UK. *Journal of Wind Engineering and Industrial Aerodynamics*, 115. C. 104 - 111. ISSN: 0167-6105

<https://doi.org/10.1016/j.jweia.2013.01.007>

---

**Reuse**

Items deposited in White Rose Research Online are protected by copyright, with all rights reserved unless indicated otherwise. They may be downloaded and/or printed for private study, or other acts as permitted by national copyright laws. The publisher or other rights holders may allow further reproduction and re-use of the full text version. This is indicated by the licence information on the White Rose Research Online record for the item.

**Takedown**

If you consider content in White Rose Research Online to be in breach of UK law, please notify us by emailing [eprints@whiterose.ac.uk](mailto:eprints@whiterose.ac.uk) including the URL of the record and the reason for the withdrawal request.

Elsevier Editorial System(tm) for Journal of Wind Engineering & Industrial  
Aerodynamics  
Manuscript Draft

Manuscript Number:

Title: Estimating the potential yield of small wind turbines in urban areas: A case study for Greater London, UK.

Article Type: Full Length Article

Keywords: wind; energy; micro-generation; urban; boundary layer; roughness length; morphology

Corresponding Author: Dr Daniel Robert Drew,

Corresponding Author's Institution: University of Reading

First Author: Daniel Robert Drew

Order of Authors: Daniel Robert Drew; Janet F Barlow; Tim T Cockerill

## \*Highlights (for review)

- We derive a new map of annual mean wind speeds across Greater London
- Results used to assess the best location for small wind turbine installations
- Small wind turbines perform better towards outskirts of Greater London
- Distance from city centre is a useful parameter for siting small wind turbines
- Very few sites identified which meet threshold wind speed outlined in literature

1 **Estimating the potential yield of small wind turbines in urban areas: A case study**  
2 **for Greater London, UK.**

3 D.R. Drew<sup>a</sup>, J.F. Barlow<sup>a</sup>, T.T. Cockerill<sup>b</sup>

4 <sup>a</sup> Department of Meteorology, University of Reading, UK

5 <sup>b</sup> Centre for Environmental Policy, Imperial College London, UK

6 **Abstract**

7 To optimise the placement of small wind turbines in urban areas a detailed understanding of the  
8 spatial variability of the wind resource is required. At present, due to a lack of observations, the  
9 NOABL wind speed database is frequently used to estimate the wind resource at a potential site.  
10 However, recent work has shown that this tends to overestimate the wind speed in urban areas. This  
11 paper suggests a method for adjusting the predictions of the NOABL in urban areas by considering  
12 the impact of the underlying surface on a neighbourhood scale. In which, the nature of the surface is  
13 characterised on a 1 km<sup>2</sup> resolution using an urban morphology database.

14 The model was then used to estimate the variability of the annual mean wind speed across Greater  
15 London at a height typical of current small wind turbine installations. Initial validation of the results  
16 suggests that the predicted wind speeds are considerably more accurate than the NOABL values. The  
17 derived wind map therefore currently provides the best opportunity to identify the neighbourhoods  
18 in Greater London at which small wind turbines yield their highest energy production.

19 The results showed that the wind speed predicted across London is relatively low, exceeding 4 ms<sup>-1</sup>  
20 at only 27% of the neighbourhoods in the city. Of these sites less than 10% are within 10 km of the  
21 city centre, with the majority over 20 km from the city centre. Consequently, it is predicted that  
22 small wind turbines tend to perform better towards the outskirts of the city, therefore for cities  
23 which fit the Burgess concentric ring model, such as Greater London, 'distance from city centre' is a  
24 useful parameter for siting small wind turbines. However, there are a number of neighbourhoods  
25 close to the city centre at which the wind speed is relatively high and these sites can only been  
26 identified with a detailed representation of the urban surface, such as that developed in this study.

27 **KEYWORDS:** wind, energy, micro-generation, urban, boundary layer, roughness length, morphology

28 **1. Introduction**

29 To reduce the carbon emissions associated with the electricity delivered to the built environment,  
30 the UK government has developed a number of schemes to incentivise the growth of micro-  
31 generation technologies, including the Low Carbon Buildings Programme, the Code for Sustainable  
32 Homes and the Feed-in tariffs Order (Allen et al., 2008; Walker, 2011). As a result there has been an  
33 increase in the number of micro-generation technology installations in the UK, including micro-wind  
34 turbines (Bergman and Jardine, 2009; RenewableUK, 2011). However, a number of high profile field  
35 studies have shown that currently, small wind turbines installed in urban areas in the UK generally  
36 produce less energy than expected prior to installation. This has raised doubts about their potential,

37 both in the context of the financial benefits to the owner and with respect to decarbonising the UK  
38 energy supply (Encraft, 2009; James et al., 2010).

39 The literature suggests the reason for the poor performance is twofold: Firstly, the majority of the  
40 turbines installed in urban areas are designed without taking into account the complex nature of the  
41 wind resource at roof level. Consequently, a number of recent studies have focused on designing  
42 wind turbines specifically for urban applications (Booker et al., 2010; Henriques et al., 2009; Muller  
43 et al., 2009). Secondly, due to the difficulty estimating the wind resource in an urban area there has  
44 been poor placement of the turbines. To optimise the placement of the turbines an accurate method  
45 of assessing the variability of the wind resource across a wide urban area is required.

46 For large-scale wind turbine installations extensive wind monitoring is generally conducted to  
47 identify potential sites, however, due to financial constraints, this is rarely possible for small urban  
48 installations. Bahaj et al. (2007) and Allen et al. (2008) assessed the performance of small wind  
49 turbines in urban areas using wind speed data collected at Met Office weather stations however  
50 such data are relatively scarce in urban areas. Consequently, to identify the best sites over a wide  
51 area there is a reliance on modelled wind speed data. There are several sources of wind resource  
52 information available in the UK. In recent years, the DECC wind speed database and Carbon Trust  
53 wind speed estimator have been the most commonly used tools. However, recent studies have  
54 shown there can be large inaccuracies in their predictions, particularly in urban areas (Encraft, 2009;  
55 James et al., 2010).

56 This paper aims to provide guidance for optimising the placement of small wind turbines in urban  
57 areas by developing an improved method of estimating the wind resource across a wide urban area.  
58 The first section discusses the tools currently used to estimate the wind resource at a potential site.  
59 This is followed by a discussion of the method developed in this study. Finally, the method has been  
60 applied to estimate the wind speed across Greater London, from which the best sites for small wind  
61 turbines (from an energy production perspective) have been identified.

## 62 **2. Current Methods of estimating the wind resource in urban areas**

63 The DECC wind speed database has been widely used by installers and planners for a number of  
64 years to identify sites for the installation of micro-wind turbines (James et al., 2010; Walker, 2011). It  
65 provides estimates of the annual mean wind speed at three heights (10, 25 and 45 m) on a 1 km  
66 resolution. It was produced by a mass consistent flow model, NOABL (Numerical Objective Analysis  
67 of the Boundary Layer), which interpolated wind speed data from 56 weather stations across the UK  
68 assuming a uniform surface (Burch and Ravenscroft, 1992). However, studies have shown that the  
69 database tends to overestimate the wind speed at urban locations (James et al., 2010). At 16 of the  
70 25 sites considered in the Warwick wind trials the measured wind speed was over 40% lower than  
71 the NOABL prediction (Encraft, 2009). The inaccuracy of the database is indicative of the simplicity of  
72 the model and in particular the lack of representation of the impact of the underlying urban surface  
73 on the flow.

74 An urban surface affects the flow over a range of horizontal spatial scales: city scale (up to 10 or 20  
75 km), neighbourhood scale (up to 1 or 2 km) and street scale (less than 100 to 200 m) (Britter and  
76 Hanna, 2003). At the street scale, interacting wakes are introduced by individual surface obstacles,  
77 hence at close proximity to buildings the nature of the flow is dependent on a number of local

78 surface parameters such as building size, shape and orientation. This region of the urban boundary  
79 layer is known as the roughness sublayer and extends from the surface up to a height of  
80 approximately 2-5 times the mean building height (Roth, 2000).

81 Blackmore (2008) used wind tunnel experiments to consider flow around a range of different  
82 building designs and configurations in the roughness sublayer (i.e. on the street scale). Mertens et al.  
83 (2003) and Watson and Harding (2007) performed a similar analysis using CFD simulations. The  
84 results from these studies provide useful guidance as to the best location for small wind turbines  
85 above a specific building or within a given street. However due to cost and time constraints, it is not  
86 possible to apply this method to consider the wind speed across a wide urban area. Nevertheless, by  
87 considering the flow patterns in the roughness sublayer a modified NOABL estimation tool has been  
88 developed. The Micro-generation Installation Standard: MIS 3003 applies correction factors to the  
89 NOABL wind speed based on turbine height and urbanisation of the site, termed NOABL-MCS (MIS,  
90 2009). While this approach considers the impact of the surface on the flow in the roughness  
91 sublayer, it does not consider the impact which occurs on larger scales. Consequently, James et al.  
92 (2010) showed that despite the adjustment, the NOABL-MCS still generally overestimates the wind  
93 resource in urban areas.

94 The region directly above the roughness sublayer is known as the inertial sublayer (ISL), which  
95 extends up to a height of approximately  $0.1z_i$ , where  $z_i$  is the height of the UBL. In this region the  
96 flow around individual buildings is averaged out, therefore the boundary layer has adapted to the  
97 integrated effect of the underlying urban surface (city scale). The wind speed in neutral conditions  
98 therefore is considered to be horizontally homogeneous and increases logarithmically with height

$$U(z) = \frac{u_*}{\kappa} \ln\left(\frac{z-d}{z_0}\right) \quad (1)$$

99 where  $U$  is the wind speed at a height  $z$ ,  $u_*$  is the friction velocity and  $\kappa$  is von Karman's constant.  
100 The roughness length,  $z_0$ , provides a measure of the drag exerted on the wind by the underlying  
101 surface, with a higher value indicating greater drag. When the surface obstacles are densely packed,  
102 such as in an urban area, they can be considered collectively as a canopy of mean height,  $h$ . This  
103 results in a vertical displacement to the wind profile, known as the displacement height,  $d$ . While  
104 equation 1 is strictly only valid in the ISL, Cheng and Castro (2002) and Coceal et al. (2006) have  
105 shown that it is also approximately satisfied down to the top of the canopy layer for spatially  
106 averaged flow.

107 The impact of the urban surface on the flow in the ISL forms the basis on the Carbon Trust wind  
108 resource assessment tool. The tool enables a user to specify their postcode and the proposed height  
109 of the turbine to obtain an estimate of the annual mean wind speed. The model is based on a wind  
110 climatology which has uniform validity across the country, derived from the National Climate  
111 Information Centre (NCIC) dataset. This is adjusted to the hub height of the turbine assuming a  
112 logarithmic wind profile and the presence of a blending height  $l_b$  (Best et al., 2008). Below  $l_b$  the  
113 wind profile is governed by the local surface characteristics,  $z_{0local}$  and  $d_{local}$ , while above  $l_b$  the wind  
114 profile is governed by the effective roughness of a number of surfaces  $z_{0eff}$ . Due to the increased  
115 consideration of the impact of the surface on the flow, the Carbon Trust tool generally provides  
116 more accurate predictions of the wind speed in urban areas than NOABL. However, a field trial  
117 carried out by the Energy Saving Trust showed that the tool tends to underestimate the wind

118 resource with an error of up to 20% of the measured wind speed at some sites (Energy Saving Trust,  
119 2009).

## 120 2.1 Internal Boundary Layer Approach

121 When flow encounters a change in surface roughness, such as a boundary between a rural and an  
122 urban area, it has to adjust to the new surface characteristics. Elliott (1958) and Panofsky and Dutton  
123 (1984) showed that the impact of the new surface gradually propagates upwards and a new  
124 boundary layer begins to grow, called an Internal Boundary Layer (IBL). Within the IBL, the wind  
125 profile is governed by the local surface characteristics, whereas above the height of the IBL, the wind  
126 profile remains characteristic of the upwind surface.

127 Mertens (2003) and Heath et al. (2007) considered the growth of an IBL at the boundary between a  
128 rural and urban surface to estimate the wind speed in an urban area from a reference rural wind  
129 speed. However both studies assumed a uniform roughness length for the whole urban area. In  
130 reality, while urban surfaces are very different from the surrounding rural surfaces, they are not  
131 internally uniform. Typically, because of common use, neighbourhoods (up to 1 or 2 km) tend to  
132 exhibit reasonably uniform surface characteristics (e.g. residential, industry, commercial, parkland).  
133 However variability of the surface on this scale has not been considered when estimating the wind  
134 speed in urban areas, therefore there is a clear need to develop a method of estimating the  
135 variability of the wind resource across an urban area on a neighbourhood scale.

## 136 3. Development of a new wind speed estimation method

137 This study uses the IBL approach outlined in Mertens (2003) to estimate the wind speed across  
138 Greater London taking into account the variability of the urban surface on a neighbourhood scale.  
139 The derived wind data was then combined with the characteristics of a number of small wind  
140 turbines to estimate the neighbourhoods across the city at which their energy production is  
141 greatest.

### 142 3.1 Neighbourhood scale variability

143 To represent the nature of the surface on a neighbourhood scale, Greater London was divided into 1  
144  $\text{km}^2$  gridboxes. Each gridbox was then characterised by an estimate of  $z_0$  and  $d$ . A common approach  
145 of estimating the magnitude of  $z_0$  and  $d$  over a wide area is to use land use as a proxy (Barlow et al.,  
146 2008; Boehme and Wallace, 2008; Rooney, 2001). However, the problem for those interested in  
147 urban areas is that land use categories are usually very broad as they have to cover all types of land  
148 use (Britter and Hanna, 2003). For example, there are only two urban categories (urban and  
149 suburban) in the land use data used by the Carbon Trust model. A further problem with this  
150 approach is the assumption that pre-determined surface parameter values are applicable to  
151 different surfaces (i.e. all city centre surfaces are assigned the same  $z_0$  value). In reality, the surface  
152 characteristics of one urban surface are likely to be different from that of another and consequently  
153 there can be large variability in the magnitude of the surface parameters (Wieringa, 1993).

154 More precise estimates of  $z_0$  and  $d$  can be made using information about the size and spacing of the  
155 buildings, this is known as a morphological approach (Britter and Hanna, 2003). This study has  
156 estimated the magnitude of  $z_0$  and  $d$  using expressions derived by Macdonald et al. (1998)

$$\frac{z_0}{h} = \left(1 - \frac{d}{h}\right) \exp \left\{ - \left[ 0.5\beta \frac{C_D}{\kappa^2} \left(1 - \frac{d}{h}\right) \lambda_F \right]^{-0.5} \right\} \quad (2)$$

$$\frac{d}{h} = 1 + A^{-\lambda_P} (\lambda_P - 1) \quad (3)$$

157 where  $C_D$  is the drag coefficient of a single obstacle,  $A$  is a coefficient derived from experimental  
 158 evidence and  $\beta$  is a parameter which modifies the drag coefficient to a value more appropriate to  
 159 the particular configuration of obstacles. For this study, these values were taken to be,  $\beta=0.55$ ,  
 160  $A=3.59$  and  $C_D=1.2$ .

161 The expressions are dependent on three building morphology parameters,  $h$  the mean building  
 162 height,  $\lambda_p$  the plan area ratio (the ratio of the total plan area of the surface obstacles to the total  
 163 plan area) and  $\lambda_f$  the frontal area ratio. These parameters were computed for Greater London on a 1  
 164  $\text{km}^2$  resolution as part of the LUCID project (Evans, 2009). Even though  $\lambda_f$  was only derived for two  
 165 wind directions  $180^\circ$  (Southerly) and  $270^\circ$  (Westerly), Evans (2009) showed that the frontal area for  
 166 a particular wind direction is almost identical to the value for the opposite direction, irrespective of  
 167 building shape. Consequently, the magnitude of the roughness length calculated for westerly flow  
 168  $z_0(270)$  can be considered to be equivalent to that for easterly flow  $z_0(90)$  (similarly  $z_0(180) \approx$   
 169  $z_0(360)$ ).

170 Figure 1 shows that the derived displacement height tends to decrease with distance from the city  
 171 centre. At the city centre, where the buildings are relatively tall and densely packed, the  
 172 displacement height peaks at a magnitude of 19.5 m, which equates to  $0.8h$ . In the surrounding  
 173 suburban region, where the buildings tend to be shorter and less densely packed, the magnitude of  
 174  $d$  is lower, generally between 2 and 4 m. Figure 2 shows a similar relationship is displayed for the  
 175 roughness length for both wind directions,  $z_0$  peaks in the city centre (1.4 m for Westerly flow and  
 176 1.3 for Southerly flow) and tends to decrease to a minimum value on the outskirts. Padhra (2010)  
 177 suggested that the symmetry of the surface parameter plots shows that the spatial structure and  
 178 organisation of Greater London fits the concentric ring model proposed by Burgess (1924). However,  
 179 the figures also show that there are some regions of low  $z_0$  and  $d$  relatively close to the city centre,  
 180 these areas are generally parkland (such as Hyde Park, Regents Park and Richmond Park).

### 181 3.2 Internal Boundary Layer Model

182 By considering the growth of an IBL at a roughness change boundary, Mertens (2003) showed that  
 183 the wind speed,  $U$ , in an urban area can be estimated from a reference upwind rural wind speed  $U_A$ ,  
 184 (measured at a height  $z_A$ ) from

$$U(z) = \frac{\left( \ln \left[ \frac{\delta - d_1}{z_{01}} \right] \ln \left[ \frac{z - d_2}{z_{02}} \right] \right)}{\left( \ln \left[ \frac{z_A - d_1}{z_{01}} \right] \ln \left[ \frac{\delta - d_2}{z_{02}} \right] \right)} U_A(z_A) \quad (4)$$

185 where  $z_{01}$  and  $z_{02}$  are the roughness lengths and  $d_1$  and  $d_2$  are the displacement heights of the  
 186 upwind and downwind surfaces respectively, and  $\delta$  is the height of the internal boundary layer given  
 187 by

$$\delta(x) = 0.28z_{02} \left[ \frac{x}{z_{02}} \right]^{0.8} \quad (5)$$

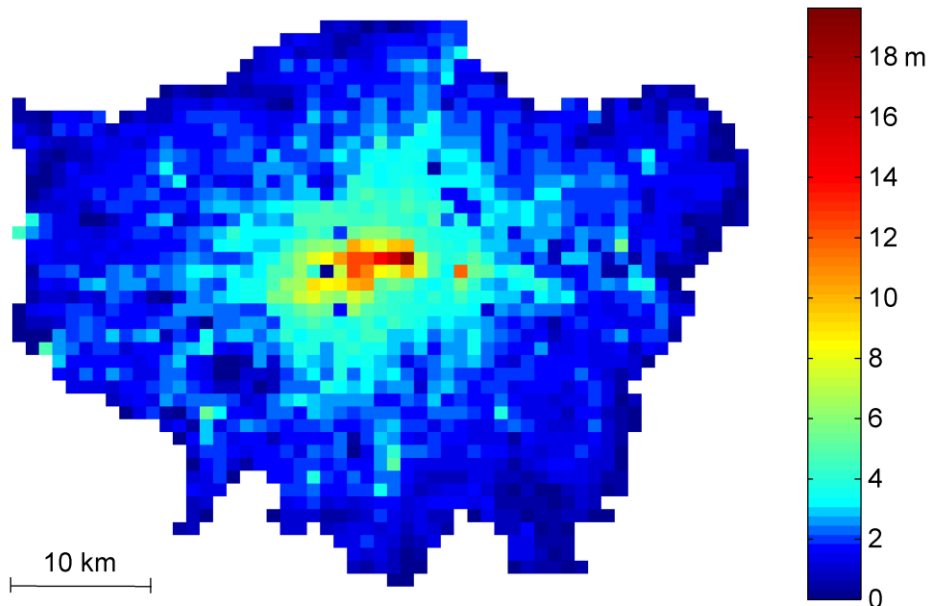
188 where  $x$  is the distance from the roughness change boundary (Elliott, 1958).

189 While Mertens (2003) assumed that a single IBL grows at the rural/urban boundary, this study  
 190 assumes that an IBL develops at the boundary between neighbourhoods of different roughness.  
 191 Equation 4 is therefore used to estimate the annual mean wind speed of each gridbox for each of  
 192 the 4 wind directions. As the wind speed calculated using equation 4 is dependent on the distance  
 193 from the roughness change boundary,  $x$ , the wind speed was calculated at a range of  $x$  values (at 50  
 194 m intervals from 50 – 950 m therefore  $n=19$ ). The gridbox mean wind speed,  $U$  is then calculated  
 195 from

$$U(z) = \frac{1}{n} \sum_{i=1}^n u_i(z) \quad (6)$$

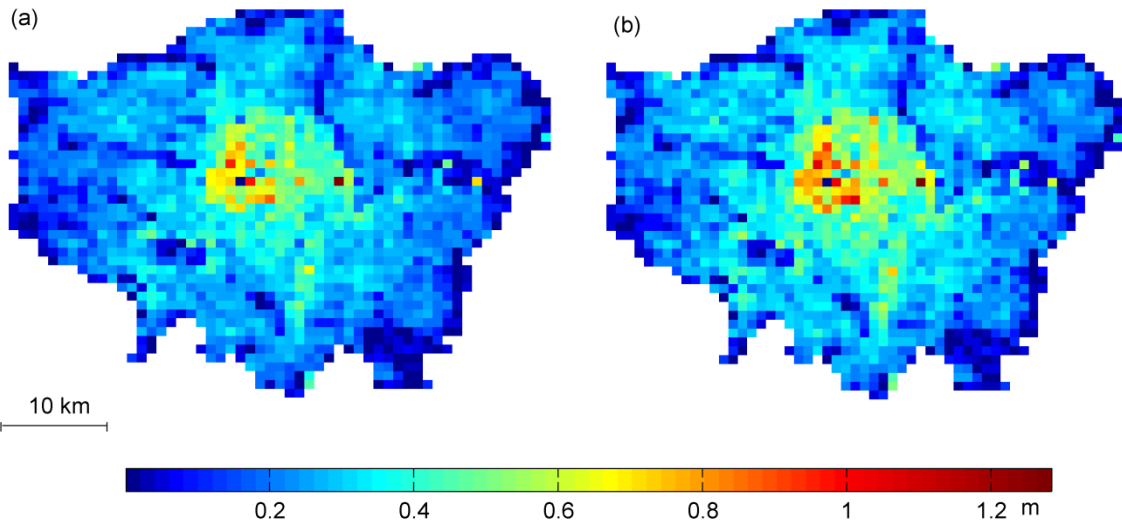
196 To apply the IBL formula for the first gridbox within the city boundary, a reference rural wind speed  
 197 is required. This has been sourced from the NOABL wind speed database; this approach is consistent  
 198 with that of Heath et al. (2007). For the downstream gridboxes, the mean wind speed derived for  
 199 the previous gridbox is used as the reference wind speed.

200 To obtain an estimate of the overall annual mean wind speed for each gridbox, the wind speed for  
 201 each of the 4 directions has been weighted based on the frequency of the wind from each direction  
 202 measured at the Met Office weather station at Heathrow between 1990 and 2011 (located on the  
 203 Western outskirts of Greater London at 51.479, -0.449) (UK Meteorological Office, 2012).



204

205 **Figure 1 Displacement height (m) of Greater London derived from urban morphology database on a 1 km<sup>2</sup>**  
 206 **resolution.**



207

208 **Figure 2 Roughness length (m) derived from urban morphology on a 1 km resolution (a) southerly/northerly**  
 209 **flow (b) westerly/easterly flow.**

### 210 3.3 Performance of small wind turbines

211 The model was used to estimate the annual mean wind speed at a hub height typical of that  
 212 recommended for a number of rooftop turbines,  $z_{hub}$ . This was taken to be either 5 m above the  
 213 mean building height or 10 m for the sites at which  $h=0$  (i.e. no buildings). To estimate the potential  
 214 energy production of a wind turbine at each gridbox, a Weibull distribution has been assumed to  
 215 represent the variability of the hourly mean wind speed.

216 The Weibull probability density function is given by

$$f(v) = \left(\frac{k}{C}\right) \left(\frac{v}{C}\right)^{k-1} \exp\left[-\left(\frac{v}{C}\right)^k\right] \quad (7)$$

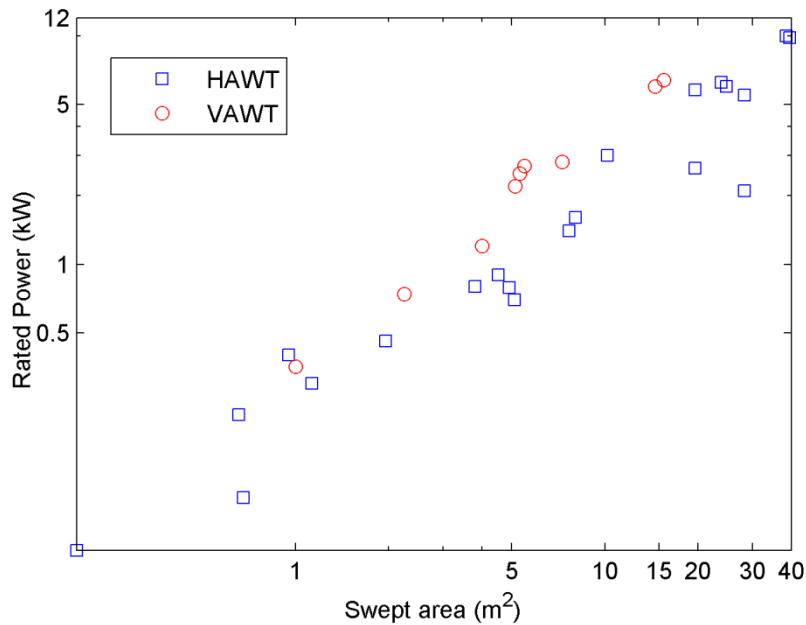
217 where  $C$  and  $k$  are known as the scale and shape parameters respectively. This study assumes that  
 218 the wind speed for each gridbox fits a Rayleigh distribution, which is a special case of the Weibull  
 219 distribution, which occurs when  $k=2$  (Lun and Lam, 2000; Ramrez and Carta, 2005).

220 The annual energy production of a range of different small wind turbines was estimated at each  
 221 gridbox by combining the turbine's power output  $P(v)$ , (given by the power curve) with the Weibull  
 222 probability density function for all of the velocities within the operating range of the turbine

$$E = t \int_{v_{cut-in}}^{v_{cut-out}} P(v) f(v) dv \quad (8)$$

223 where  $t$  is the number of hours in a year.

224 Figure 3 shows the details of the 30 wind turbines considered in this study. The selection was  
 225 considered to represent the full range of systems currently available in the UK, both in terms of size  
 226 and design. The figure shows that 21 horizontal axis wind turbines (HAWTs) and 9 Vertical axis wind  
 227 turbines (VAWTs) with a rated power ranging from 0.056 to 9.8 kW have been considered.



228

229

**Figure 3 Details of the swept area and the rated power of the 30 turbines used in this study.**

230

**4. Wind resource results**

231

Figure 4 shows the predicted annual mean wind speed at  $z_{hub}$  is generally higher on the outskirts of Greater London than the city centre region. The wind speed was estimated to be highest on the south west outskirts, with a value of approximately  $5 \text{ ms}^{-1}$ . The lowest wind speeds were predicted in and around the city centre, with a magnitude of  $3.3 \text{ ms}^{-1}$ . However, there are some regions close to the city centre with a relatively high wind speed which therefore do not fit this relationship, these equate to the regions of low  $z_0$  and  $d$  values (i.e. such as Hyde Park and Richmond Park).

237

**4.1 Validation**

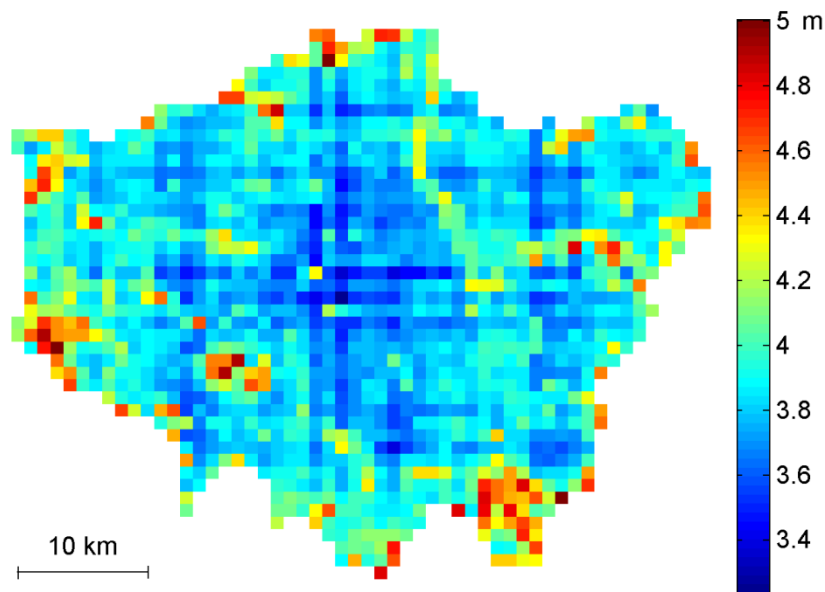
238

Ideally the mean wind speed predictions of the model would be validated with measured data. However, of the 8 Met Office weather stations in Greater London with wind speed observations only two are currently operational and hold wind data for a minimum of 10 years; Heathrow and Northolt, both of which are located towards the outskirts of the region. For both sites, the model has been used to estimate the wind speed at a height of 10 m, the results have then been compared with the measured wind speed data averaged over the period 2000-2010. To have further confidence in the model, the predictions have also been compared with the predictions of the NOABL wind speed database and Carbon Trust tool.

246

At both sites, the method outlined in this study produces a prediction of the annual mean wind speed within one standard deviation of the measured value. At the Northolt site the model overestimates the measured annual mean wind speed by only 3%. In comparison, the NOABL database overestimates by 27% and the Carbon Trust tool underestimates by 16%. A similar result was shown at the Heathrow site, with the model overestimating the annual mean wind speed by only 1% in comparison to an 18% overestimate by NOABL and 31% underestimate by the Carbon Trust tool.

252



253

254 **Figure 4 The annual mean wind speed, U, at zhub, based on the NOABL climatology upstream.**

255 **5. Implications for small wind turbines in urban areas**

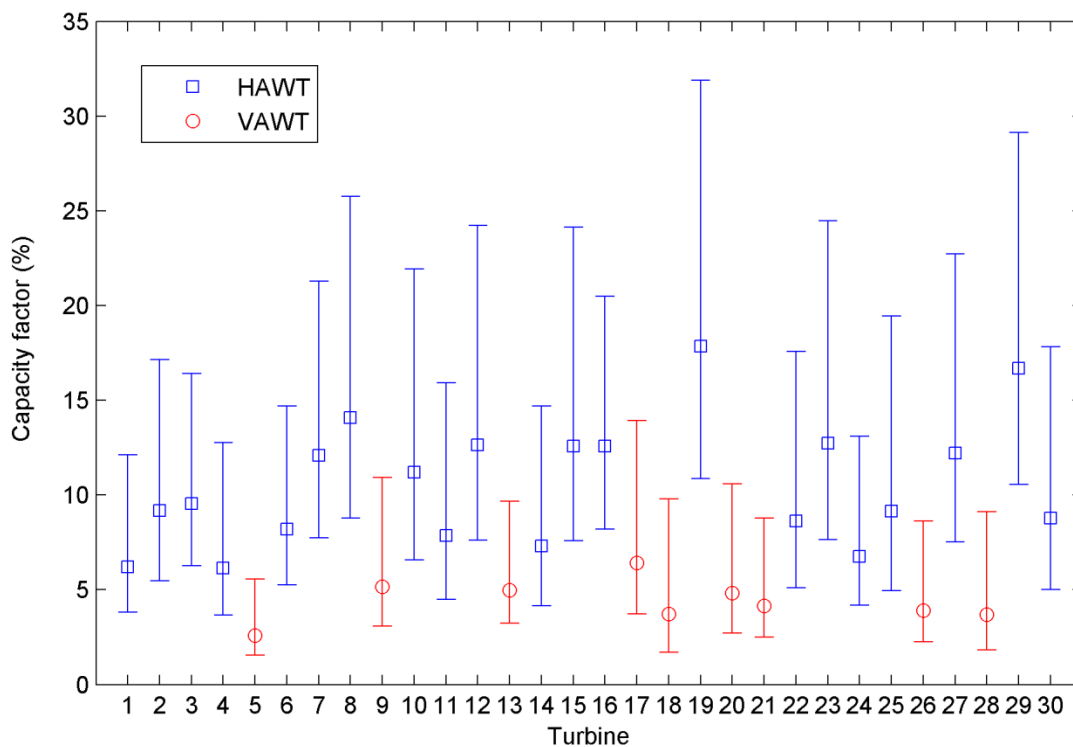
256 The wind map of Greater London has been used to estimate the potential annual energy production  
 257 of 30 small wind turbines at each of the 1 km neighbourhoods across Greater London (using the  
 258 method outlined in section 3.3). To allow comparison between the turbines, the performance has  
 259 been expressed in the form of a capacity factor. This is defined as the ratio of the actual energy  
 260 production in a given period, to the hypothetical maximum possible.

261 **5.1 Using the new wind map to investigate the performance of small wind turbines in Greater**  
 262 **London**

263 Figure 5 provides an analysis of the magnitude of the capacity factor for the 30 turbines, estimated  
 264 for each gridbox across the 1650 km<sup>2</sup> of Greater London. It shows there is large variability in the  
 265 annual energy production of the different turbines across the city, with the HAWTs generally  
 266 performing better. For all 9 VAWTs the median capacity factor does not exceed 6.4%, with a mean  
 267 value of 4.4%. In contrast, the median capacity factor is below this value for only two of the HAWTs  
 268 and the mean value over the 21 turbines is 10.6%. This result is largely due to the higher cut-in wind  
 269 speed of the VAWTs. The figure also shows that there is not a clear trend between turbine size and  
 270 the predicted median capacity factor.

271 In general, the performance of the turbines across Greater London is relatively poor compared to  
 272 large wind turbines in open areas, with the median capacity factor exceeding 15% for only two  
 273 turbines (turbine 19 and 29). Further analysis showed that for all gridboxes, these two turbines were  
 274 predicted to produce the highest capacity factors. This suggests that, assuming the power curves are  
 275 accurate, of the turbines considered one of these two turbines should be selected. Figure 5 also  
 276 shows that there is large variability in the magnitude of the capacity factor of each turbine,  
 277 indicating that the turbine performance varies significantly from one location within an urban area

278 to another. This is also seen in figure 6 which shows the mean capacity factor averaged across all 30  
 279 turbines for each 1 km<sup>2</sup>. These results imply that as expected the siting of a small wind turbine is  
 280 important.

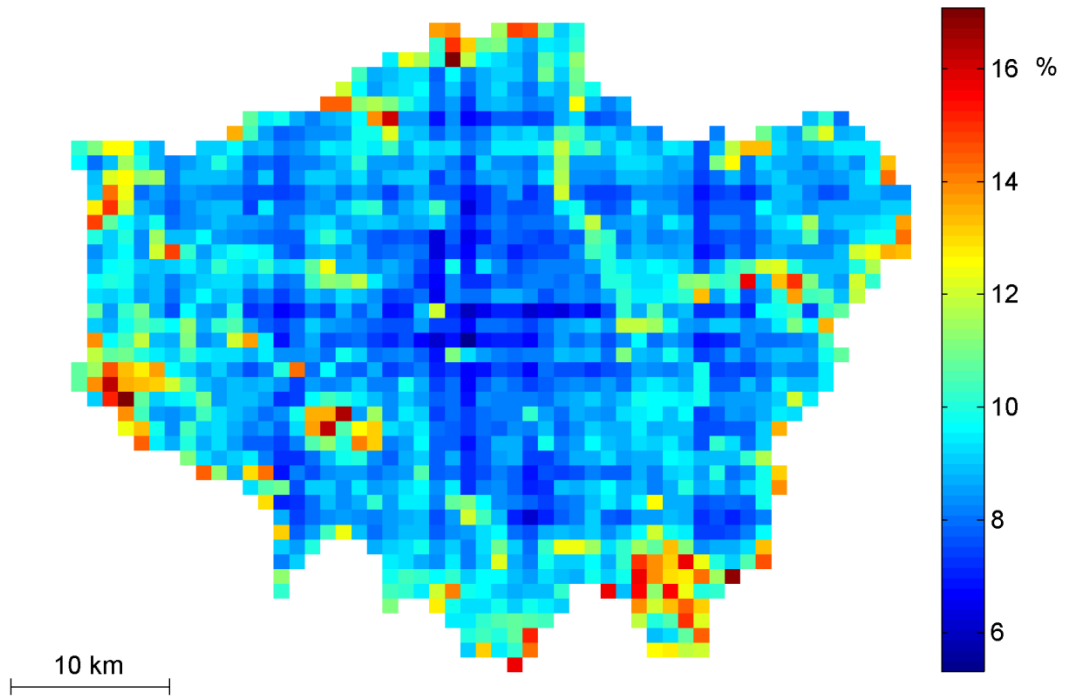


281

282 **Figure 5 Estimated capacity factor for 30 turbines across Greater London, if installed at zhub. Median,**  
 283 **minimum and maximum values across the 1650 1 km<sup>2</sup> neighbourhoods are represented, with the turbines**  
 284 **ordered by increasing rated power.**

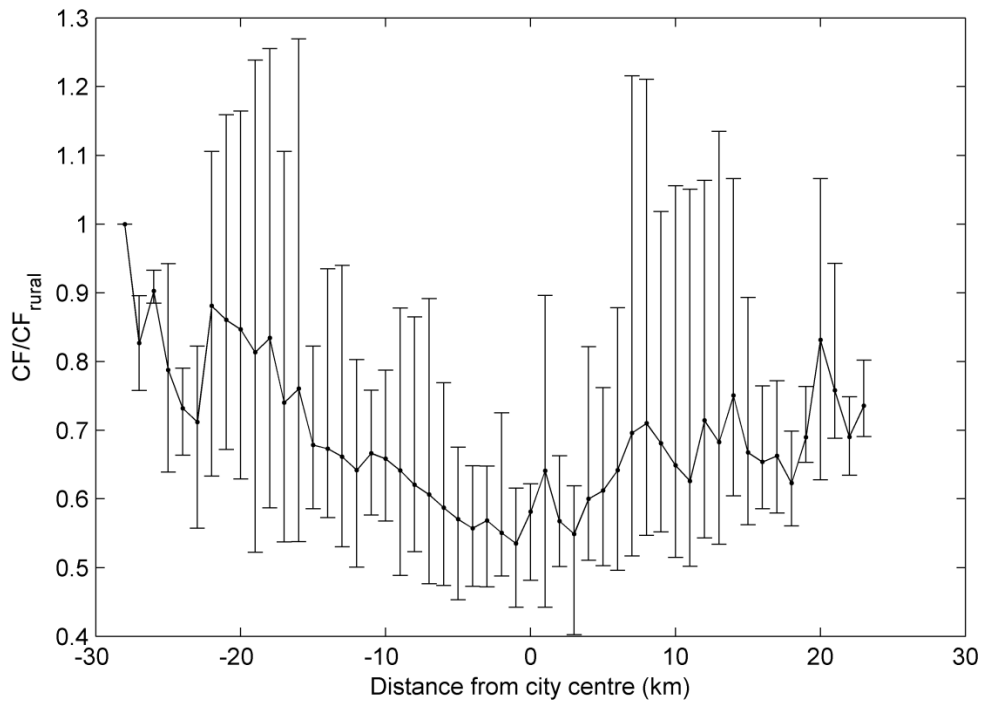
285 5.2 How does energy production vary with location?

286 The energy production of the turbines tends to increase with distance from the city centre, (due to  
 287 the increase in wind speed). To explore this relationship further the magnitude of the mean capacity  
 288 factor (across 30 turbines) along 15 transects (from 0 to 360° every 24°) through Greater London has  
 289 been considered. Figure 7 shows the mean capacity factor averaged across the 15 transects as a  
 290 function of distance from the city centre, as well as the minimum and maximum values. The values  
 291 have been normalised by the mean capacity factor for the rural gridbox at the start of each transect.  
 292 The figure shows that the mean capacity factor generally peaks towards the outskirts of the city  
 293 before decreasing to a minimum value in the city centre. A similar relationship is shown for the  
 294 minimum value. These results suggest that for cities which fit the Burgess concentric ring model,  
 295 such as Greater London, 'distance from city centre' is a useful parameter for siting small wind  
 296 turbines. However, figure 7 also shows that there is large variability in the maximum value of the  
 297 mean capacity factor across the transects; there are sites close to the city centre at which the mean  
 298 capacity factor is relatively high. This suggests that to identify the best sites for small wind  
 299 (in terms of energy production) further siting parameters, such as  $z_0$  and  $d$ , are required on a  
 300 neighbourhood scale.



301

302 **Figure 6 Mean capacity factor of the 34 turbines at zhub for each 1 km<sup>2</sup> neighbourhood in Greater London.**



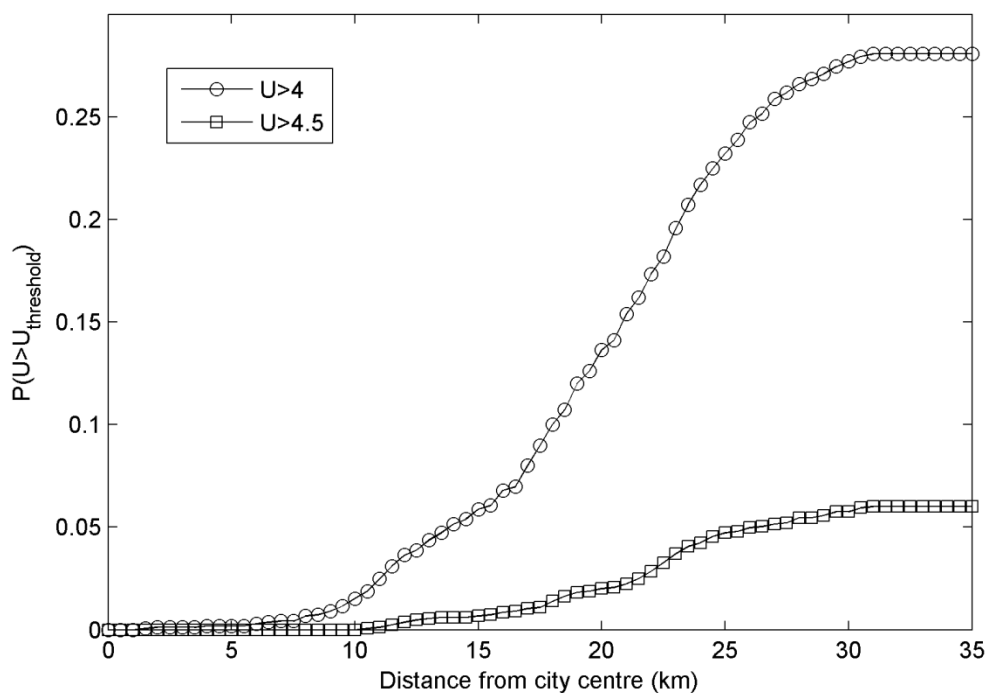
303

304 **Figure 7 Mean capacity factor of 34 turbines estimated at zhub averaged along 15 transects through Greater**  
 305 **London. The values have been normalised by the mean capacity factor at the rural site at the start of each**  
 306 **transect.**

307

308 5.3 What proportion of sites meet the RenewableUK criteria?

309 RenewableUK guidance states that it is generally worthwhile installing a small wind turbine at a site  
310 with a mean wind speed of  $4\text{--}5\text{ ms}^{-1}$  (RenewableUK, 2012). This study predicts that the mean wind  
311 speed at  $z_{\text{hub}}$  exceeds the threshold of  $4\text{ ms}^{-1}$  at only 28% of the  $1\text{ km}^2$  neighbourhoods in Greater  
312 London. Of these neighbourhoods, the majority are located towards the outskirts of the city, figure 8  
313 shows that 50% are over 22 km from the city centre. Furthermore, the wind speed exceeds the  
314 threshold at only two gridboxes within a distance of 5 km of the city centre (which correspond to  
315 Hyde Park). The figure also shows that only 6% of the neighbourhoods have an annual mean wind  
316 speed in excess of  $4.5\text{ ms}^{-1}$ , all of which are at a distance of more than 10 km from the city centre.  
317 Finally, if the threshold wind speed is taken to be  $5\text{ ms}^{-1}$ , small wind turbines could only be installed  
318 in two neighbourhoods in Greater London, both of which are on the western outskirts of the city.



319

320 **Figure 8 Probability of finding a neighbourhoods for which the predicted annual mean wind speed at  $z_{\text{hub}}$**   
321 **exceeds the threshold wind speed as a function of distance from the city centre.**

322 **5. Conclusions**

323 Urban areas have largely been considered poor sites for small wind turbines, this conclusion has  
324 generally been drawn from observations of the wind resource at point locations. However, there has  
325 been little work optimising the placement of the turbines. This study has developed a method for  
326 estimating the variability of the annual mean wind speed across an urban area by considering the  
327 impact of the surface on a neighbourhood scale, in order to identify the best sites for small wind  
328 turbine installations.

329 The method has been applied to estimate the wind resource across Greater London, UK. Due to a  
330 lack of measured wind data in the city, there has been limited validation of the model's predictions.  
331 However, for the two sites with wind data available, the predictions were shown to be within one

332 standard deviation of the measured wind speed data and considerably more accurate than both of  
333 the alternative site assessment tools (NOABL and Carbon Trust tool). These results suggest that the  
334 wind map developed in this study therefore presents the best opportunity to assess the  
335 performance of small wind turbines in Greater London.

336 The results show that generally the wind speed across London is relatively low. Of the 1650 1 km<sup>2</sup>  
337 neighbourhoods within the city, only 28% exceed the guideline threshold wind speed of 4 ms<sup>-1</sup> at  
338 turbine hub height, outlined by RenewableUK. Of these sites less than 10% are within 10 km of the  
339 city centre, with the majority over 20 km from the city centre. The performance of small wind  
340 turbines therefore tends to be better on the outskirts of the city, particularly in the boroughs of  
341 Hounslow in the west and Bromley in the south east. Consequently, for cities which fit the Burgess  
342 concentric ring model, such as Greater London, 'distance from city centre' is a useful parameter for  
343 siting small wind turbines. However, there are some regions close to the city centre at which the  
344 wind speed is relatively high and these sites can only be identified by representing the urban surface  
345 on a neighbourhood scale.

346 The results also show that for each neighbourhood there is large variability in the performance of  
347 the different turbines, with the HAWTs generally performing better than VAWTs. Averaged across all  
348 neighbourhoods in London, the median capacity factor does not exceed 6.4% for any of the VAWTs.  
349 In contrast, the median capacity factor is below this value for only two of the HAWTs.

350 The approach outlined in this study, has thus far only been applied to Greater London, but could be  
351 replicated for all cities for which urban morphology data is available. It could therefore provide a  
352 useful tool for optimising the placement of small wind turbines in urban areas for the whole of the  
353 UK. The model however does not consider the impact of individual obstacles on the flow and  
354 therefore does not consider the variability of the wind speed at close proximity to buildings. The  
355 results can therefore be used to identify the best neighbourhoods for small wind turbines, in terms  
356 of the wind resource. However, to identify the best locations within each region, scaling factors need  
357 to be applied to the wind speed to account for the impact of individual buildings on the flow.

### 358 **Acknowledgements**

359 The authors acknowledge the financial support from the Engineering and Physical Sciences Research  
360 Council (EPSRC) Doctoral training grant. Thanks to Sylvia Bohnenstengel for the derived products  
361 from the Virtual London dataset.

362

363

364

365

366

367

368

369 **Figure Captions**

370 Figure 1 Displacement height (m) of Greater London derived from urban morphology database on a  
371 1 km<sup>2</sup> resolution.

372 Figure 2 Roughness length (m) derived from urban morphology on a 1 km resolution (a)  
373 southerly/northerly flow (b) westerly/easterly flow.

374 Figure 3 Details of the swept area and the rated power of the 30 turbines used in this study

375 Figure 4 The annual mean wind speed, U, at z<sub>hub</sub>, based on the NOABL climatology upstream

376 Figure 5 Estimated capacity factor for 30 turbines across Greater London, if installed at z<sub>hub</sub>. Median,  
377 minimum and maximum values across the 1650 1 km<sup>2</sup> neighbourhoods are represented, with the  
378 turbines ordered by increasing rated power.

379 Figure 6 Mean capacity factor of the 34 turbines at z<sub>hub</sub> for each 1 km<sup>2</sup> neighbourhood in Greater  
380 London.

381 Figure 7 Mean capacity factor of 34 turbines estimated at z<sub>hub</sub> averaged along 15 transects through  
382 Greater London. The values have been normalised by the mean capacity factor at the rural site at  
383 the start of each transect.

384 Figure 8 Probability of finding a neighbourhoods for which the predicted annual mean wind speed at  
385 z<sub>hub</sub> exceeds the threshold wind speed as a function of distance from the city centre.

386

387

388

389

390

391

392

393

394

395

396

397

398

399

400

401 **References**

- 402 Allen, S., Hammond, G., & McManus, M. (2008). Energy analysis and environmental life cycle  
403 assessment of a micro-wind turbine. *Power and Energy*, 669-684.
- 404 Bahaj, A., Myers, L., & James, P. (2007). Urban energy generation: Influence of micro-wind turbine  
405 output on electricity consumption in buildings. *Energy and Buildings*, 154-165.
- 406 Barlow, J., Rooney, G., von Huenerbein, S., & Bradley, S. (2008). Relating Urban Surface-Layer  
407 Structure to Upwind Terrain for the Salford Experiment (Salfex). *Boundary Layer  
408 Meteorology*, 173-191.
- 409 Bergman, N., & Jardine, C. (2009). *Power from the people: Domestic microgeneration and the low  
410 carbon buildings programme*. Environmental Change Institute.
- 411 Best, M., Brown, A., Clark, P., Hollis, D., Middleton, D., Rooney, G., et al. (2008). *Small-scale wind  
412 energy: Part 1- A review of existing knowledge*. Met Office.
- 413 Blackmore, P. (2008). *Siting micro-wind turbines on house roofs*. BRE.
- 414 Boehme, T., & Wallace, A. (2008). Hindcasting Hourly Wind Power Across Scotland Based on Met  
415 Station Data. *Wind Energy*, 233-244.
- 416 Booker, J., Mellor, P., Wrobel, R., & Drury, D. (2010). A compact, high efficiency contra-rotating  
417 generator suitable for wind turbines in the urban environment. *Renewable Energy*, 2027-  
418 2033.
- 419 Britter, R., & Hanna, S. (2003). Flow and dispersion in urban areas. *Annual Review of Fluid  
420 Mechanics*, 469-496.
- 421 Burch, S., & Ravenscroft, F. (1992). *Computer modelling of the UK wind energy resource: Overview  
422 report*. ETSU WN7055.
- 423 Celik, A., Muneer, T., & Clarke, P. (2007). An investigation into micro wind energy systems for their  
424 utilization in urban areas and their life cycle assessment. *Power and Energy*, 1107-1117.
- 425 Cheng, H., & Castro, I. (2002). Near-wall flow over urban-like roughness. *Boundary Layer  
426 Meteorology*, 229-259.
- 427 Coceal, O., & Belcher, S. (2004). A canopy model of the mean winds through urban areas. *Quarterly  
428 Journal of the Royal Meteorological Society*, 1349-1372.
- 429 Coceal, O., Thomas, T., Castro, I., & Belcher, S. (2006). Mean flow and turbulence statistics over  
430 groups of urban-like cubical obstacles. *Boundary Layer Meteorology*, 491-519.
- 431 DECC. (2008). *Climate Change Act*.
- 432 Elliott, W. (1958). The growth of the atmospheric internal boundary layer. *American Geophysical  
433 Union*, 1048-1054.

434 Energy Saving Trust. (2009). *Location, location, location: Domestic small-scale wind field trial report*.  
435 Energy Saving Trust.

436 Encraft. (2009). *Warwick wind trials final report*. Encraft.

437 Evans, S. (2009). *3D cities and numerical weather prediction models: An overview of the methods*  
438 *used in the LUCID project*. London: UCL Centre for Advanced Spatial Analysis.

439 Heath, M., Walshe, J. D., & Watson, S. J. (2007). Estimating the potential yield of small building  
440 mounted wind turbines. *Wind Energy*, 271-283.

441 Henriques, J., Marques da Silva, F., Estanqueiro, A., & Gato, L. (2009). Design of a new urban wind  
442 turbine airfoil using a pressure-load inverse method. *Renewable Energy*, 2728-2734.

443 James, P., Sissons, M., Bradford, J., Myers, L., Bahaj, A., Anwar, A., et al. (2010). Implications of the  
444 UK field trial of building mounted horizontal axis micro-wind turbines. *Energy Policy*, 6130-  
445 6144.

446 Lun, I., & Lam, J. (2000). A study of weibull parameters using long-term wind observations.  
447 *Renewable Energy*, 145-153.

448 Macdonald, R. W., Griffiths, R. F., & Hall, D. J. (1998). An improved method for the estimation of  
449 surface roughness of obstacle arrays. *Atmospheric Environment*, 1857-1864.

450 Masson, P. (1988). The formulation of areally-averaged roughness lengths. *Quarterly Journal of the*  
451 *Royal Meteorological Society*, 399-420.

452 Mertens, S. (2003). The energy yield of roof-mounted wind turbines. *Journal of Wind Engineering*,  
453 507-518.

454 Mertens, S., van Kuik, G., & van Bussel, G. (2003). Performance of an H-Darrieus in the skewed flow  
455 on a roof. *Solar energy engineering*, 125.

456 Microgeneration Installation Standard. (2009) MIS3003.

457 Muller, G., Jentsch, M., & Stoddart, E. (2009). Vertical axis resistance type wind turbines for use in  
458 buildings. *Renewable Energy*, 1407-1412.

459 Oke, T. (1987). *Boundary Layer Climates*. London: Routledge.

460 Padhra, A. (2010). *Estimating the sensitivity of urban surface drag to building morphology*. University  
461 of Reading: PhD Thesis.

462 Panofsky, H., & Dutton, J. (1984). *Atmospheric turbulence: models and methods for engineering*  
463 *applications*. Wiley.

464 Ramrez, P., & Carta, J. (2005). Influence of the data sampling interval in the estimation of the  
465 parameters of the weibull wind speed probability density distribution: a case study. *Energy*  
466 *Conversion and Management*, 2419-2438.

467 Rankine, R., Chick, J., & Harrison, G. (2006). Energy and carbon audit of a rooftop wind turbine.  
468 *Power and Energy*, 643-654.

469 RenewableUK. (2010). *Small Wind Systems*. Retrieved May 2012, from RenewableUK:  
470 <http://www.bwea.com/small/faq.html>

471 Ricciardelli, F., & Poliimeno, S. (2006). Some characteristics of the wind flow in the lower Urban  
472 boundary layer. *Wind Engineering and Industrial Aerodynamics*, 815-832.

473 Rooney, G. (2001). Comparison of Upwind Land-Use and Roughness Length Measured in the Urban  
474 Boundary Layer. *Boundary Layer Meteorology*, 469-486.

475 Roth, M. (2000). Review of atmospheric turbulence over cities. *Quarterly Journal of the Royal  
476 Meteorological Society*, 941-990.

477 Trust, E. S. (2009). *Location, location, location: Domestic small-scale wind field trial report*. Energy  
478 Saving Trust.

479 UK Meteorological Office. (2012). *MIDAS Land Surface Stations data (1853-current)*. NCAS British  
480 Atmospheric Data Centre.

481 Walker, S. (2011). Building mounted wind turbines and their suitability for the urban scale- A review  
482 of methods of estimating urban wind resource. *Energy and Buildings*, 1852-1862.

483 Watson, S., Infield, D., Barton, J., & Wylie, S. (2007). Modelling of the Performance of a Building-  
484 Mounted Ducted Wind Turbine. *Journal of Physics: Conference Series*.

485

486

Figure1  
[Click here to download high resolution image](#)

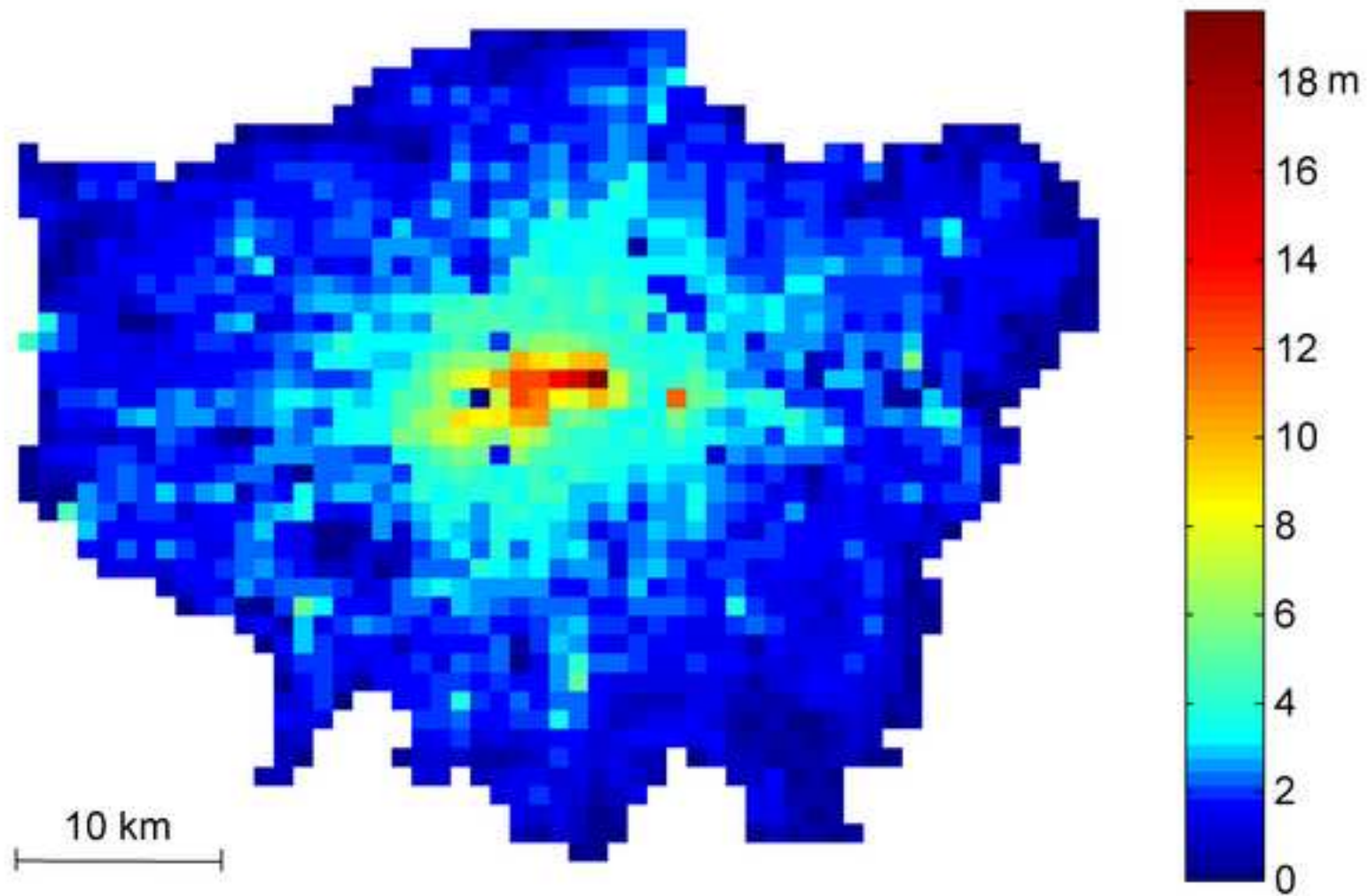


Figure2  
[Click here to download high resolution image](#)

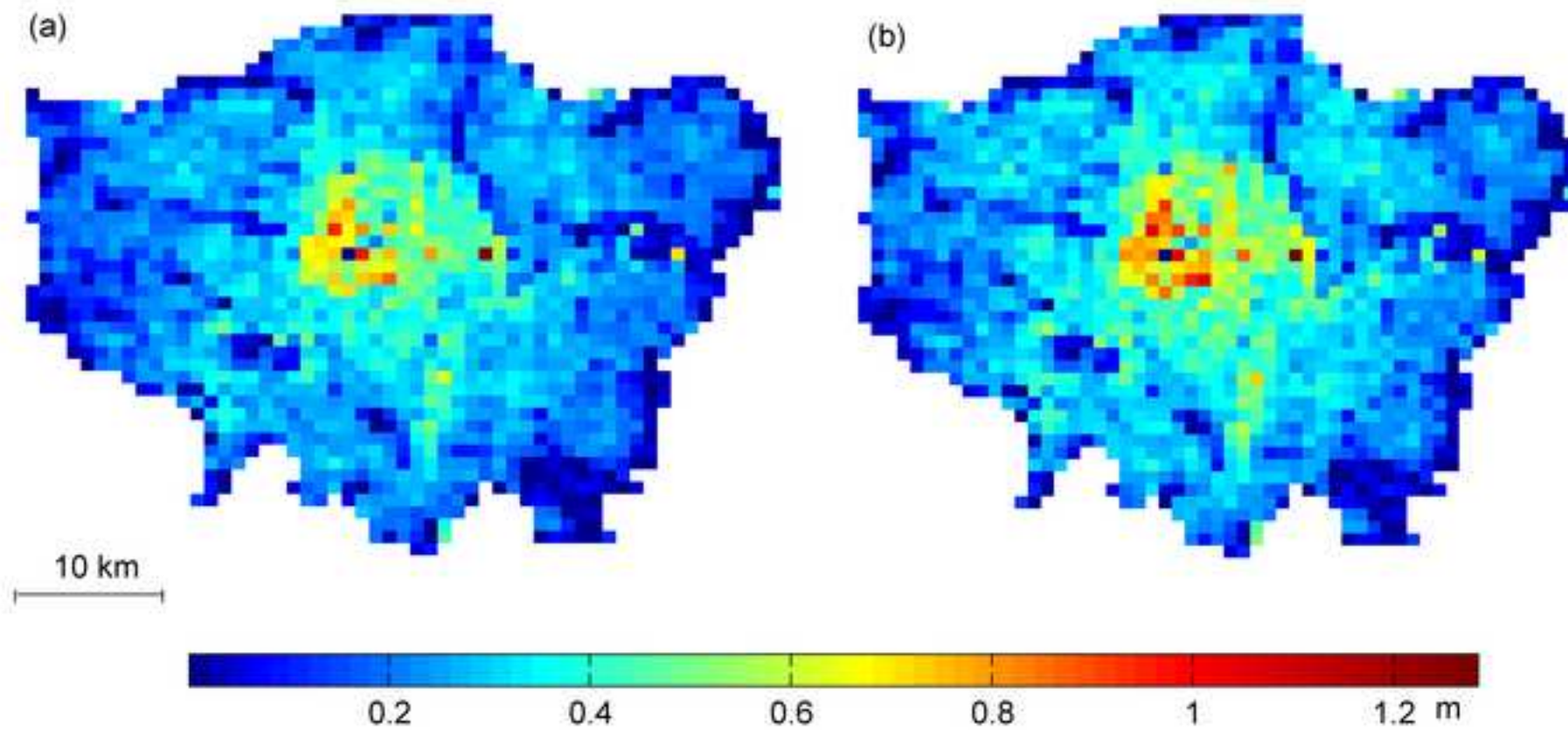


Figure3  
[Click here to download high resolution image](#)

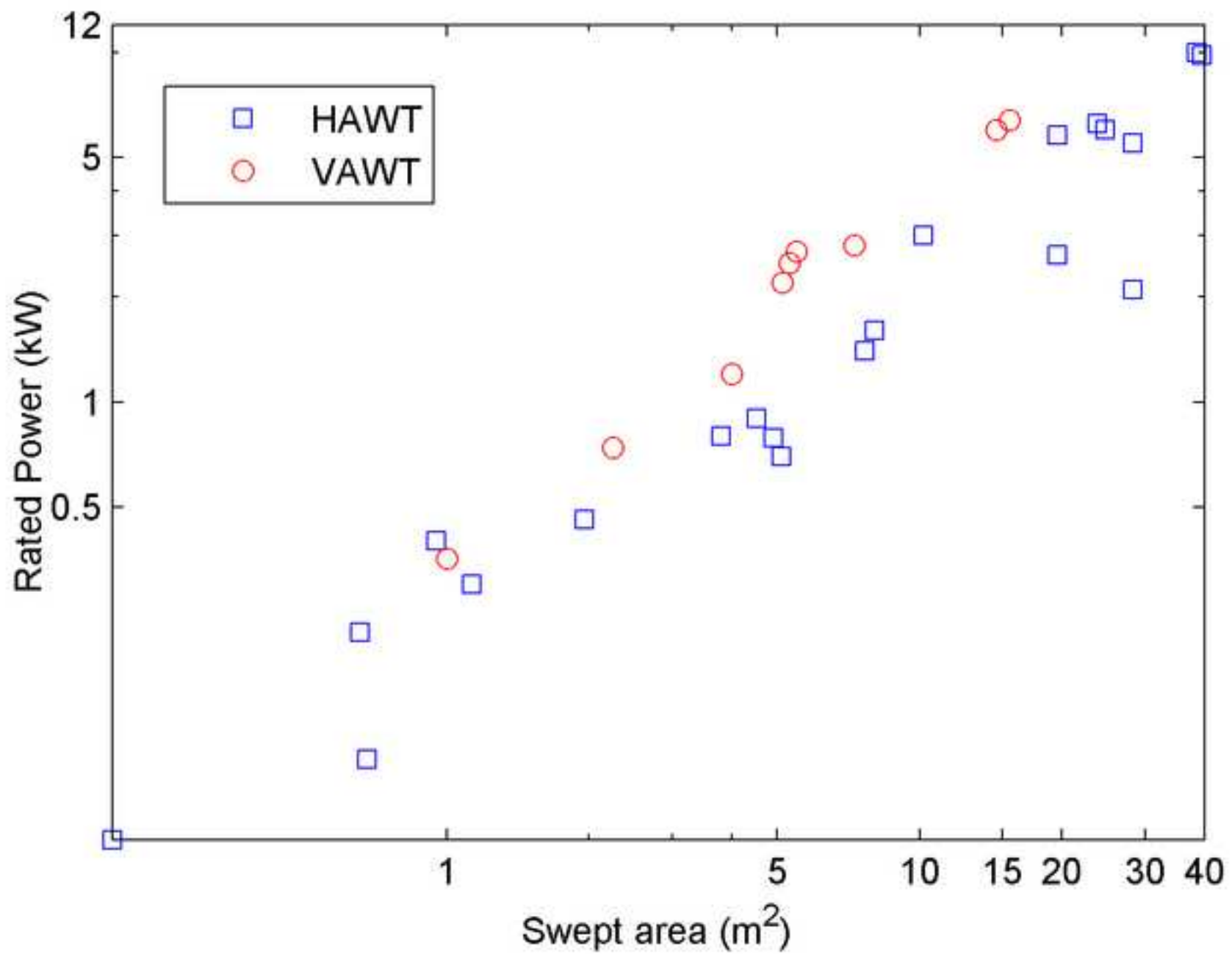


Figure4  
[Click here to download high resolution image](#)

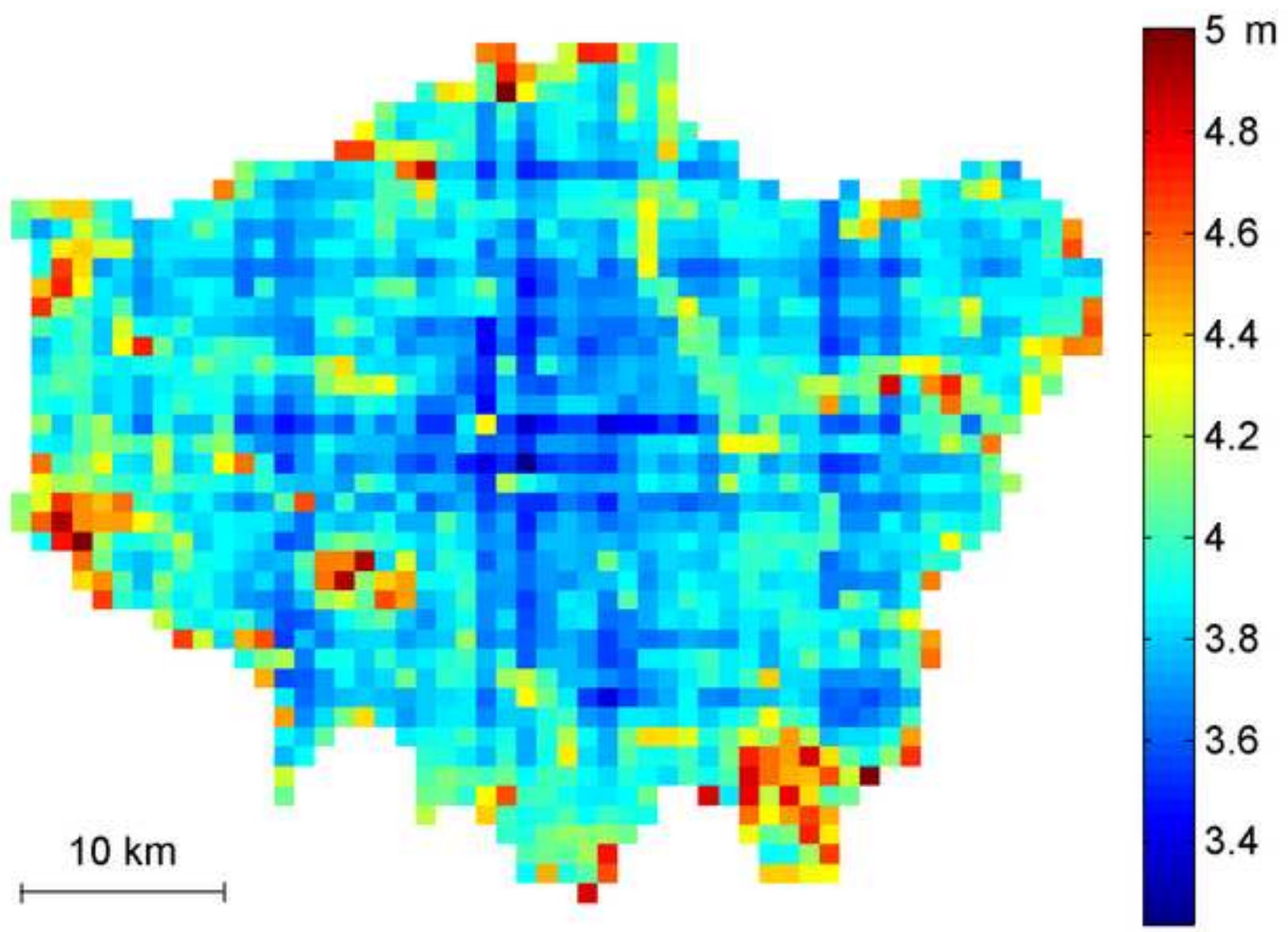


Figure5

[Click here to download high resolution image](#)

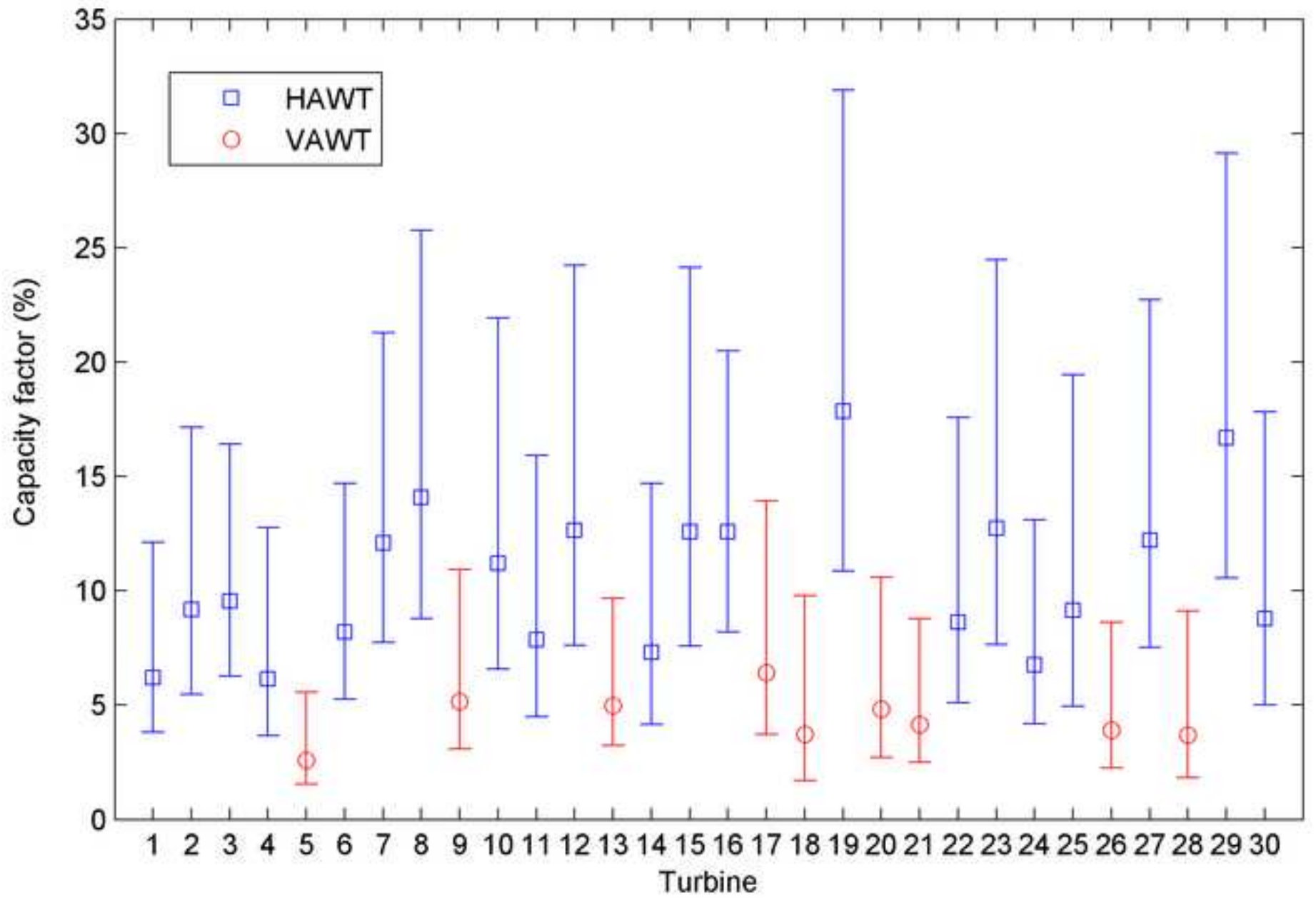


Figure6  
[Click here to download high resolution image](#)

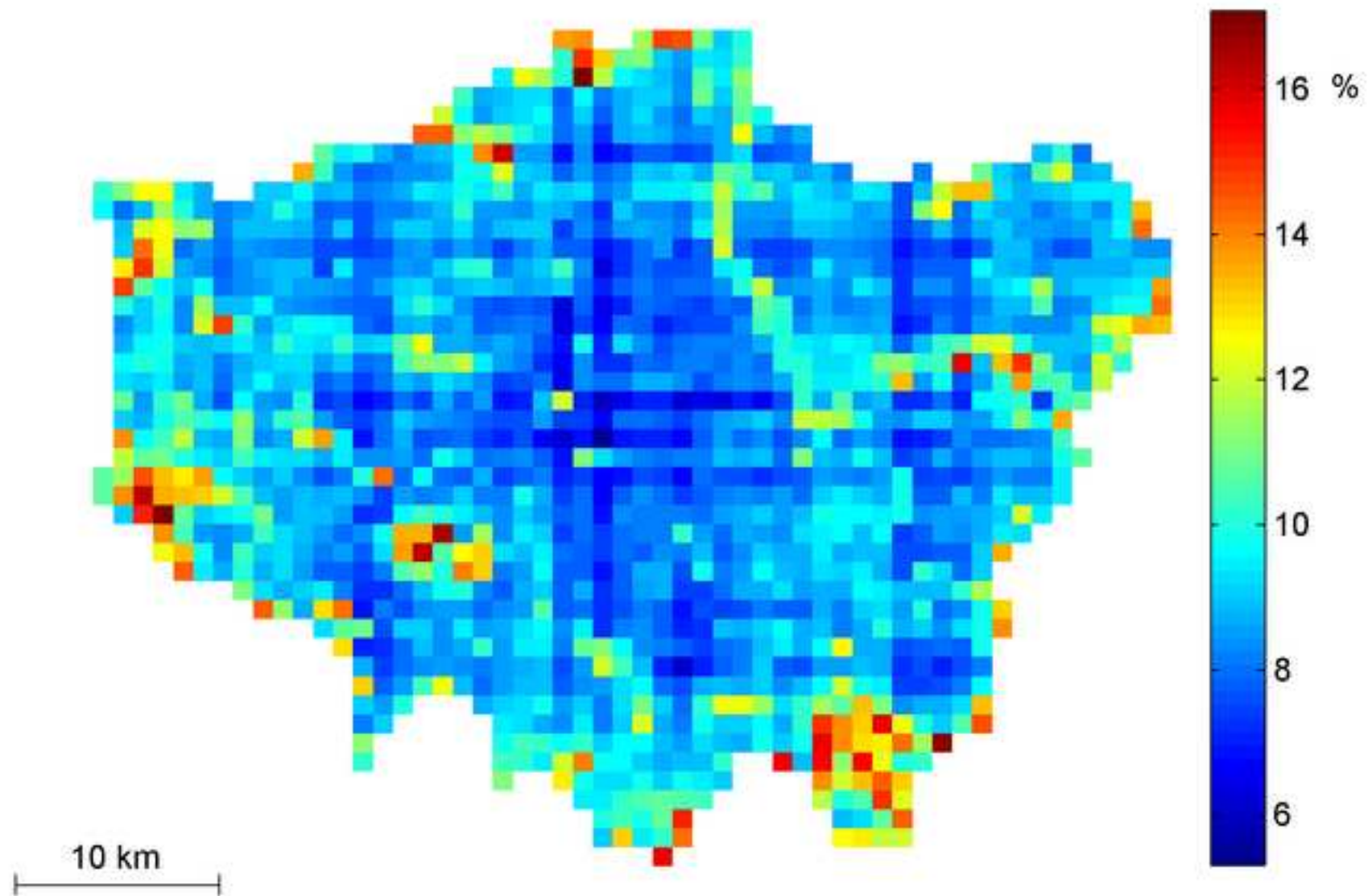


Figure7

[Click here to download high resolution image](#)

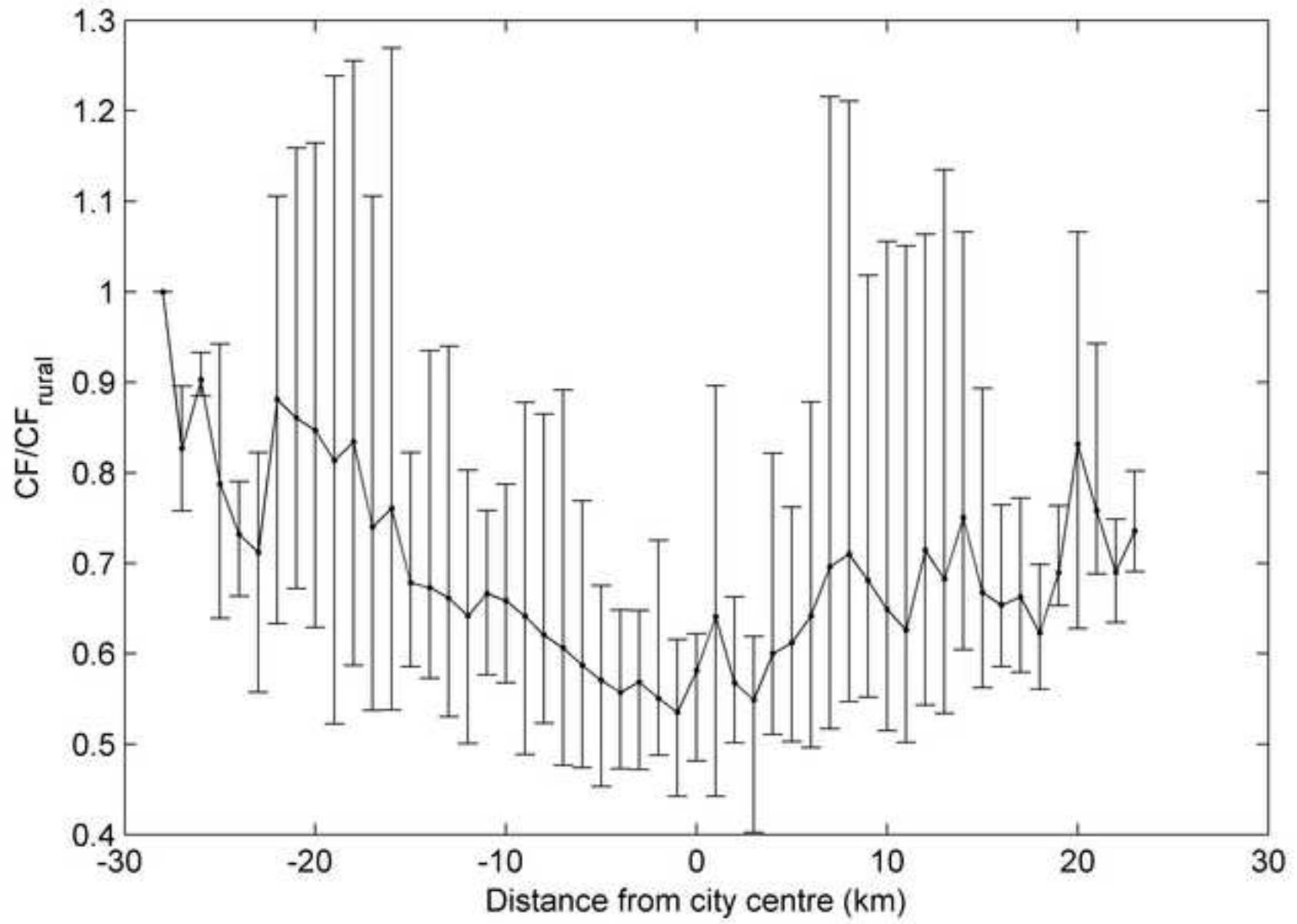


Figure8

[Click here to download high resolution image](#)

